Bragg Gratings in an Acrylate Polymer Consisting of Periodic Polymer-Dispersed Liquid-Crystal Planes

R. L. Sutherland,* L. V. Natarajan,* and V. P. Tondiglia

Science Applications International Corporation, 101 Woodman Drive, Dayton, Ohio 45431

T. J. Bunning

Materials Directorate, Wright Laboratory, Wright-Patterson Air Force Base, Ohio 45433-6533

Received June 9, 1993. Revised Manuscript Received July 22, 1993®

We report on the results of holographic studies in an acrylate photopolymer system containing a nematic liquid crystal. We demonstrate that Bragg gratings can be formed in this system and that the liquid crystal greatly enhances the diffraction efficiency. For a liquid crystal loading of 16.5 wt %, we have observed diffraction efficiencies approaching 100%. With careful control of liquid-crystal loading and rapid postcuring, we have obtained optically clear gratings of high diffraction efficiency (>80%) and narrow angular selectivity (<1°) which are stable over a period of months. Low-voltage scanning electron microscopy reveals a unique morphology for these gratings, showing that they consist of periodic polymer-dispersed liquid-crystal planes. The liquid-crystal microdroplets are confined to the Bragg planes, having a size approximately equal to one-half the grating spacing. We also observe droplet elongation and coalescence along the Bragg planes.

Introduction

Photopolymer systems have been developed for holographic applications, offering significant advantages over the conventional volume phase holographic media.[1-3] It is possible to form holographic gratings in these materials in a single-step process at relatively high speed, and the selection of different sensitizing dyes allows the use of several different optical recording wavelengths. Moreover, it is possible to control the index modulation with the addition of optical liquids. A particularly interesting modification is the addition of nematic liquid-crystal materials, which leads to the intriguing possibility of electrooptical diffractive optics.

Although liquid crystals can be added to a photopolymer as part of the postprocessing of a hologram, it is also possible to add the liquid crystal to the original prepolymer syrup. Such systems have been used to form polymer-dispersed liquid crystals (PDLCs). PDLCs consist of liquid-crystal droplets embedded in a polymer matrix.[4] These films can be switched from an opaque (scattering) state to an optically clear state by the application of an electric field. This forms the basis for display applications using these materials. We note that PDLCs can be formed from mixtures of liquid crystals and thermoset polymers or thermoplastic melts.[5] Thermally induced phase segregation has also been studied in high molecular weight liquid crystalline polymer blends.[6] These systems are not as useful for holographic applications since the polymerization is not photoinduced.

The refractive index modulation in photopolymer systems is due to spatial density or concentration variations in the resulting polymer, or spatially distributed voids. Similarly, when a liquid crystal/monomer solution containing a photoinitiator is irradiated by a spatially periodic intensity, a grating of liquid-crystal droplets will be formed. It is possible to do this using standard holographic techniques when a laser is used as the optical source for writing the gratings. Optical gratings which exhibit multiple diffraction orders (Raman-Nath regime) have been demonstrated in PDLC films.[7,8] Under conditions similar to that described above for PDLC displays, the diffraction efficiency of these gratings can be modulated by an externally applied electric field.

Several applications, such as wide angle beam deflectors and reflection filters, will require diffraction gratings operating in the Bragg regime. These gratings should have the potential of high diffraction efficiency and high angular selectivity. Fine gratings (thousands of lines per mm) for optics require very small droplets and control of droplet dispersion. Small droplets (i.e., <1 μm) generally require a fast, efficient photocure to produce rapid phase separation of the liquid crystal.

We report in this article the fabrication and characterization of holographic Bragg gratings in a novel PDLC system. To our knowledge, this is the first demonstration of Bragg gratings in this type of system. Our photopolymer-liquid crystal system allows fast, single-step recording

* To whom correspondence should be addressed.

® Abstract published in *Advance ACS Abstracts,* September 1, 1993.

(1) Whitney, D. H.; Ingwall, R. L. *Proc. Soc. Photo-Opt. Instrum. Eng.* **1990**, *1213*, 18.

(2) Weber, A. W.; Smothers, W. K.; Trout, T. J.; Mickish, D. J. *Proc. Soc. Photo-Opt. Instrum. Eng.* **1990**, *1212*, 30.

(3) Zhang, J.; Sponsler, M. B. *J. Am. Chem. Soc.* **1992**, *114*, 1506.

(4) Doane, J. W.; Vaz, N. A.; Wu, B.-G.; Zumer, S. *Appl. Phys. Lett.* **1986**, *48*, 269.

(5) West, J. L. In *Liquid-Crystalline Polymers; ACS Symp. Ser.* 435; Weiss, R. A., Ober, C. K., Eds.; American Chemical Society: Washington, DC, 1990; p 475.

(6) Zheng, J. Q.; Kyu, T. In *Liquid-Crystalline Polymers; ACS Symp. Ser. 435*; Weiss, R. A., Ober, C. K., Eds.; American Chemical Society: Washington, DC, 1990; p 458.

(7) Lackner, A. M.; Margerum, J. D.; Ramos, E.; Lim, K.-C. *Proc. Soc. Photo-Opt. Instrum. Eng* **1989**, *1080*, 53.

(8) Sutherland, R. L. *Proc. Soc. Photo-Opt. Instrum. Eng.* **1989**, *1080*, 83.

0897-4756/93/2805-1533$04.00/0

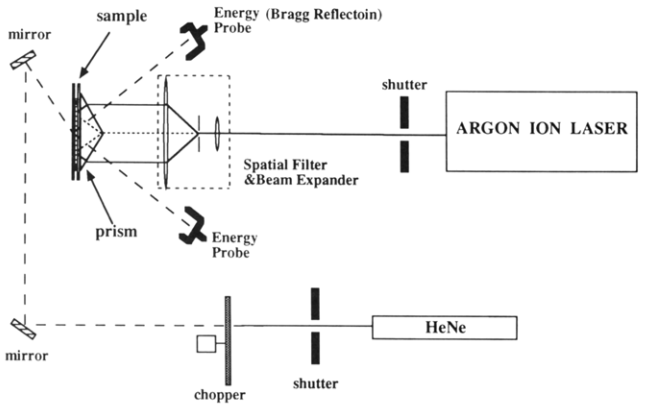

Figure 1. Holographic recording and real time optical reading experimental setup.

of optical phase gratings with spatial frequencies of the order of 2000 lines/mm and diffraction efficienices approaching 100%. The gratings formed are shown to consist of a periodic array of PDLC planes superimposed upon a polymer density grating.

Experimental Section

Materials. The recipe for the prepolymer syrup was typically a solution of the monomer dipentaerythrol hydroxy penta acrylate (DPHPA), with 10–30 wt % of the liquid crystal E7, 10 wt % of

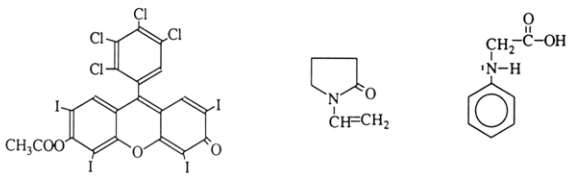

RB NVP NPG

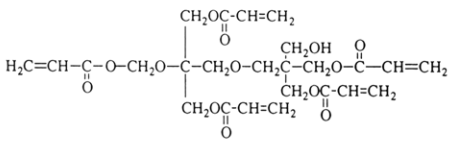

DPHPA

the cross-linking monomer *N*-vinylpyrrollidone (NVP), millimolar range by weight of the coinitiator *N*-phenylglycine (NPG), and 10^{-4} M of the photoinitiator dye Rose Bengal (RB). RB is ideally suited for holographic recording with an Ar ion laser as it displays a broad absorption spectrum with a peak molar extinction coefficient of $\sim 10^4$ M^{-1} cm^{-1} at about 490 nm. This mixture was homogenized to a viscous solution by ultrasonification and spread between glass slides with spacers of nominally 15–100-μm thickness. Preparation, mixing, and transfer of the prepolymer syrup onto the glass slides were done in the dark as the mixture is extremely sensitive to light.

Grating Formation and Characterization. The holographic recording technique is shown in Figure 1. The light source is an Ar ion laser, and although we have used all of the visible Ar ion wavelengths to record gratings, the work reported here involves the 488- and 514.5-nm lines. The beam passes through a spatial filter and is expanded. It is then passed through an aperture and centered on the apex of a 90° prism. The sample is placed in optical contact with the prism base using index matching liquids. The laser intensity was varied between 0.1 and 100 mW/cm^2, with exposure times of typically 30–120 s. Grating formation was monitored in real time using an in situ HeNe laser probe with incident angle set at the appropriate Bragg angle. After laser exposure, some samples were rapidly and completely cured by a 5-min exposure to a Blackray mercury lamp with a blue filter, while some samples were allowed to fully cure slowly under normal room lights for a period of days. Fully cured samples showed no coloration since the Rose Bengal was completely bleached in the photocuring process.

Samples were characterized for angular sensitivity and peak diffraction efficiency using several Ar ion and HeNe laser wavelengths. The morphology of the samples was investigated by low-voltage, high-resolution scanning electron microscopy (SEM) using a Hitachi 5-900 electron microscope equipped with an emission gun. The low voltage (1 keV) enabled a very thin conductive coating (1.5 nm of tungsten) to be employed. The PDLC samples were compared to samples containing no liquid crystal in the mixture.

Results and Discussion

Mechanism and Speed of Grating Formation. The mechanisms of holographic grating formation in photopolymer systems have been studied in detail.[1-3] Gratings are photochemically induced by the writing beams in the regions of constructive interference. In our photopolymer system, absorption by the photoinitiator RB results in an excited singlet state followed by fluorescence or intersystem crossing to the triplet state.[9] The RB triplet undergoes an electron-transfer reaction in which NPG functions as an electron donor, producing an NPG radical. Free radical polymerization is then initiated by the NPG radical. The presence of NVP promotes the cross-linking of the polymer chains produced. Regions in the bright fringes of the radiation interference pattern are now locked by polymerization, and a change of volume results due to shrinkage. Dark fringe regions remain as prepolymer fluid, and diffusion of molecules to the polymerized regions follows.

Polymerization leads to changes in the chemical potential of the system, increasing the miscibility gap between the liquid crystal and its host. Therefore, the liquid crystal separates as a distinct phase in submicrometer droplets in the regions of polymerization. The resulting grating is thus a superposition of a polymer density grating and a liquid-crystal droplet grating.

The effect of the liquid crystal on the diffraction efficiency is dramatic. In the pure polymer grating, the peak diffraction efficiency is typically ~1%, but never >5%. With liquid crystal loading of <20 wt %, the peak efficiency ranges from >40% to >90%, depending on the reading wavelength, polarization, and sample thickness.

Carre et al.[10] have used real time diffraction from holographic gratings to study the mechanisms and kinetics of photopolymerization reactions. The diffraction efficiency as a function of time exhibits three main regions: (1) a short induction period during which no polymerization takes place until all inhibitors, e.g., oxygen, have reacted; (2) a period of rapid photoinitiator bleaching with concomitant fast free-radical polymerization and cross-linking indicated by a rapidly increasing diffraction efficiency; (3) a plateau in the diffraction efficiency when most of the dye molecules are irreversibly bleached.

An example of such a real-time study of grating formation in our system is shown in Figure 2. The same general features described above are evident. However, the induction period in this system is very short as measurable diffraction could be observed as early as 250 ms after start of exposure. The diffraction efficiency obtainable in PDLC samples is more than a factor of ten

(9) Neckers, D. C. *J. Photochem. Photobiol. A, Chem.* **1989**, *47*, 1.
(10) Carre, C.; Lougnot, D. J.; Fouassier, J. P. *Macromolecules* **1989**, *22*, 791.

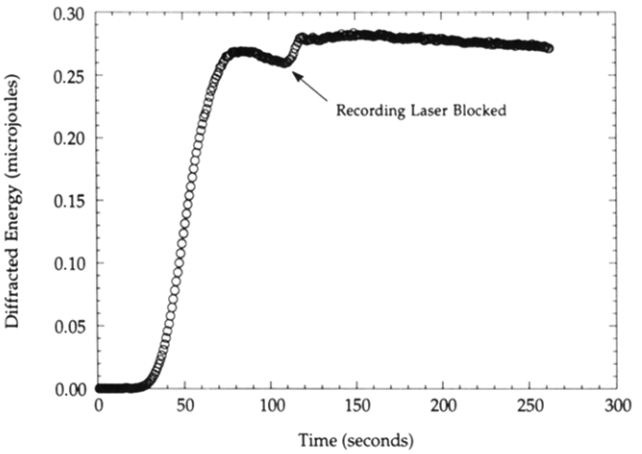

Figure 2. Diffraction efficiency as a function of time at 633 nm in a PDLC sample. The recording wavelength was 488 nm, and time $t = 0$ corresponds to the initial irradiation of the sample at this wavelength.

larger than in pure polymer samples. Therefore, the early portion of the curve in Figure 2 may be indicative of the nucleation time for phase separation of the liquid crystal microdroplets. The growth of the grating reaches a maximum around 80 s. When the laser is blocked, a small increase in diffraction efficiency is seen followed by a plateau. In the dark, living polymer chains continue to grow for some time before they terminate by radical trapping or interaction with another radical.[11] This is indicated by the plateau region. It is important to note that this plateau does not indicate a saturation of the index modulation. We have successfully written multiple gratings in samples following the initial grating growth period.

The rapid cross-linking of this photopolymer system as well as the anisotropic curing of the holographic process do not allow sufficient time for the liquid crystal microdroplets to grow to micrometer size. Indeed, as we will show below, the droplets are trapped in the polymerized regions. However, slow postcuring of underdeveloped samples with high liquid-crystal content (>30 wt %) has led to the formation of large micrometer size droplets superimposed on the PDLC grating. We have observed these large birefringent droplets under a polarized optical microscope and also in SEM. Like ordinary PDLCs, these droplets lead to a hazy (scattering) appearance of the gratings and can be reversibly switched (cleared) by the application of heat or an electric field. Through careful control of liquid-crystal loading and postcuring, we have been able to consistently obtain optically clear diffraction gratings.

Morphology. SEM photographs of an in plane (surface) view of PDLC gratings are shown in Figure 3. The photographs are of the same sample, but under different magnifications. This holographic grating was written at 488 nm with an intensity of 5 mW/cm^2, with a 60-s exposure and a 5-min postcure under a UV lamp. The liquid-crystal loading was 16.5% by weight.

Liquid-crystal droplets are clearly evident and are regularly aligned along Bragg planes. We note that the droplets do not overlap distinguishable Bragg planes and have a size roughly equal to one-half of the grating spacing. The grating spacing is approximately 0.54 μm which, as

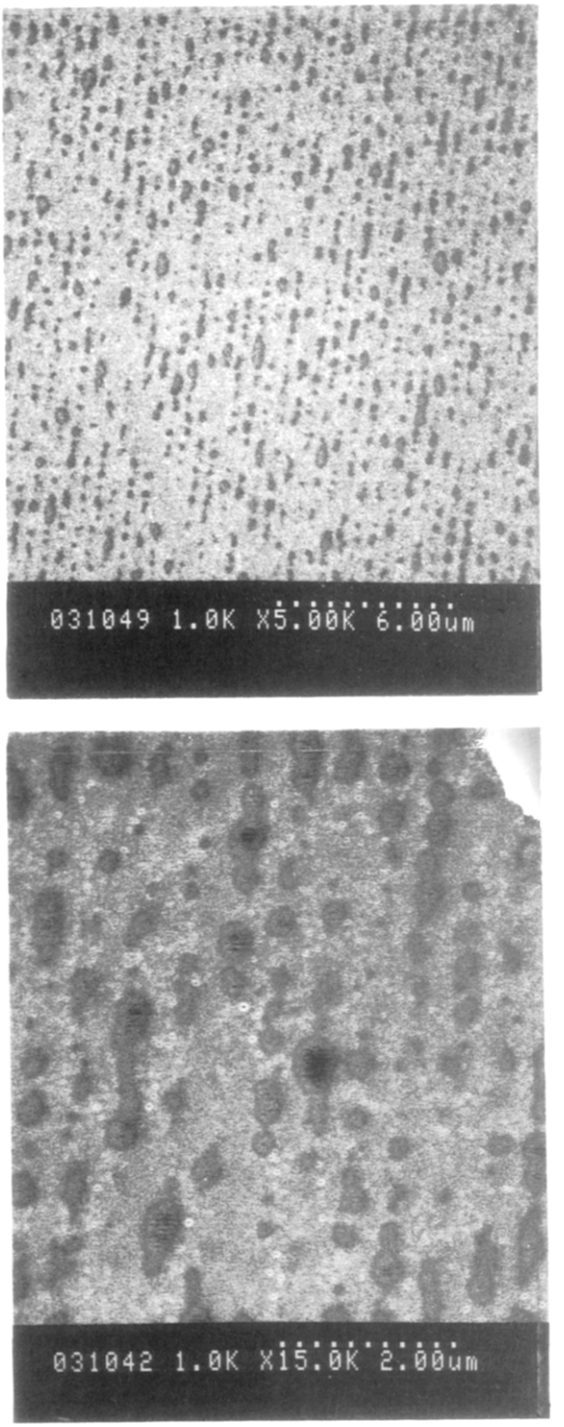

Figure 3. SEM photographs of an in plane view of a PDLC grating: (a) 5000× magnification. (b) 15 000× magnification.

we show below, is in excellent agreement with optical measurements. In the higher magnification photograph, Figure 3b, we notice that although some of droplets have an almost spherical shape, several of them are ellipsoidal with an aspect ratio of about 4:3. It is intringuing that the droplets are so confined to the Bragg planes, even to the extent that closely formed droplets have apparently coalesced. Also, the major axes of the ellipsoidal droplets are all aligned along the Bragg plane. Preliminary results of TEM (transmission electron microscopy) studies on 80-nm thin cross sections of PDLC gratings, cut perpendicular to the Bragg planes, show agreement with the SEM photographs. These give further evidence that the liquid-crystal droplets are confined to the Bragg planes,

(11) Decker, C.; Moussa, K. In *Radiation curing of polymeric materials*; *ACS Symp. Ser. 417*; Hoyle, C. E., Kinstle, J. F., Eds.; American Chemical Society: Washington, DC, 1990.

having a size approximately equal to one-half the grating spacing.

We surmise that the droplets are formed as described earlier. However, they may also be subjected to internal stresses due to the anisotropic nature of the curing in the holographic process. As regions of the material under high intensity radiation polymerize, there will be a volume shrinkage and an ensuing density gradient. This will cause monomers in the adjacent dark regions to diffuse into the bright, polymerized region creating an internal compression. This may then be responsible for the droplet elongation and coalescence. As we will discuss below, this diffusion may also lead to a density anisotropy in the Bragg planes.

The morphology evident in Figure 3 differs starkly from that of the Raman–Nath PDLC gratings which have been reported earlier. Rather than a smooth sinusoidal distribution of small droplets[8] or a periodic distribution of different droplet sizes,[7] these gratings evidently consist of periodic PDLC planes, or more correctly slabs, with droplet size uniformly equal to the slab width (i.e., one-half the grating spacing). These PDLC planes are separated by polymer planes containing no liquid-crystal droplets.

We form a crude estimate of the volume fraction of liquid-crystal droplets within the sample in the following manner. From the SEM photos we estimate that, on average, the distribution of droplets along a single Bragg plane is $N \sim 1.4/\mu m$. We ignore the coalescence of some droplets as well as their ellipticity, taking the droplets to all be spherical with an average diameter equal to $\Lambda/2$, where Λ is the grating spacing. For uniform, nearly spherical droplets, the volume fraction occupied by the droplets can be set equal to the fractional area of the droplet cross sections in the SEM photographs.[12] The droplet area is given by the average number of droplets along the Bragg plane times the average cross sectional area, divided by 2, assuming there are no droplets in planes interspersed between the Bragg planes. The volume fraction f is then the ratio of the droplet area in the Bragg plane (slab) to the area of the slab. We thus arrive at

$$f \approx \pi N \Lambda/16 \qquad (1)$$

Substituting in the numbers for N and Λ, we find $f \approx 0.15$.

We also performed volume fraction calculations from the SEM photographs using an image analysis program (Olympus Que4 System). These calculations were hampered by the somewhat poor image contrast of the SEM photographs. However, taking the average of several calculations using different photographs, magnifications, image areas, and image enhancement techniques, we arrived at a value of $f \approx 0.18$, slightly larger than the original fraction of liquid crystal in the mixture. It would thus appear that most if not all of the liquid crystal in the system phase separates as microdroplets. Previous examinations of PDLCs in photopolymer systems have indicated that the liquid-crystal microdroplets can contain a significant amount of uncured prepolymer.[13] Because our volume fraction calculations yield values of the order or larger than the original wt % of the liquid crystal, they may also indicate that the droplets contain some dissolved monomer as well. We note that these samples were cured

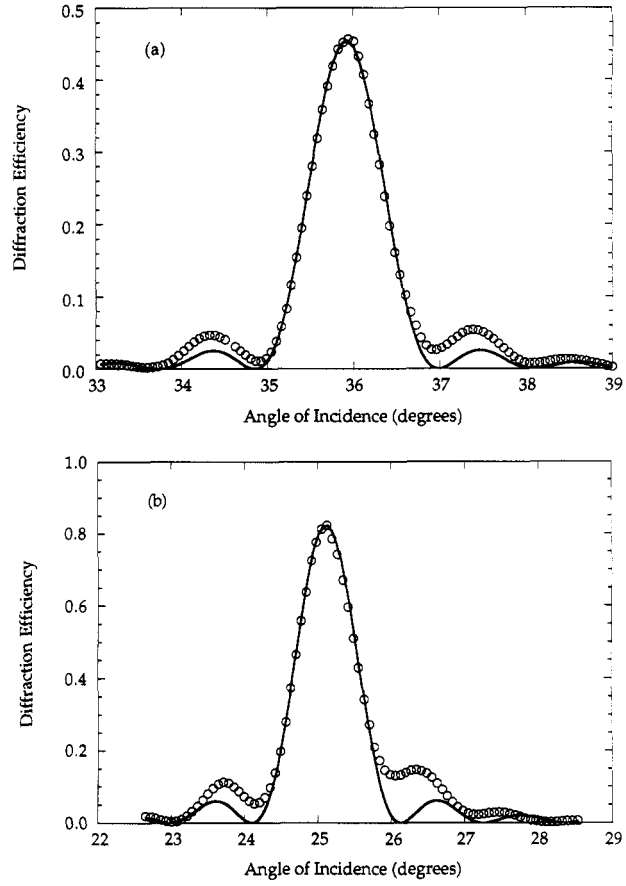

Figure 4. Angular sensitivity plots for a PLDC grating written at 488 nm. The circles are data, and the curves are theoretical fits to the data using coupled-wave theory: (a) reading wavelength = 633 nm; (b) reading wavelength = 455 nm.

at room temperature, with the rate of curing determined by the kinetics of the photochemistry and photophysics of the system. The results therefore would not necessarily be expected to agree with the volume fractions obtained with similar sized droplets in thermally cured epoxies at elevated temperatures.[12]

Diffraction Efficiency. Examples of peak diffraction efficiency and angular sensitivity obtainable with these PDLC gratings are shown in Figures 4 and 5. The grating in Figure 4 was recorded with the 488-nm line of the Ar ion laser and read with s-polarized light. In Figure 4a, the reading wavelength was 633 nm (HeNe laser), while in Figure 4b it was 455 nm (Ar ion laser). The data have been corrected for angle and polarization dependent Fresnel reflection losses. The measured (external) Bragg angles are 35.9° and 25.1°, respectively. These give grating spacings of 0.539 and 0.536 μm, both in excellent agreement with the SEM photos of these gratings. From the geometry of our recording setup, we calculate the theoretical grating spacing to be given by

$$\Lambda_t = \lambda_r/2n \cos[\alpha + \sin^{-1}(n^{-1} \cos \alpha)] \qquad (2)$$

where $\lambda_r = 488$ nm is the recording wavelength, α is the half-angle of the prism apex, and we take $n = 1.52$ for the glass prism. Using eq 2 for a 90° prism, we compute $\Lambda_t = 0.541$ μm. Hence, it appears that the rapid recording and postcuring of these samples assure that there is little shrinkage of the gratings. In fact, the Bragg angle has remained constant in these samples for months after the gratings were recorded.

(12) Montgomery, Jr., G. P.; West, J. L.; Tamura-Lis, W. *J. Appl. Phys.* **1991**, *69*, 1605.
(13) Nolan, P.; Tillin, M.; Coates, D. *Mol. Cryst. Liq. Cryst.* **1992**, *8*, 129.

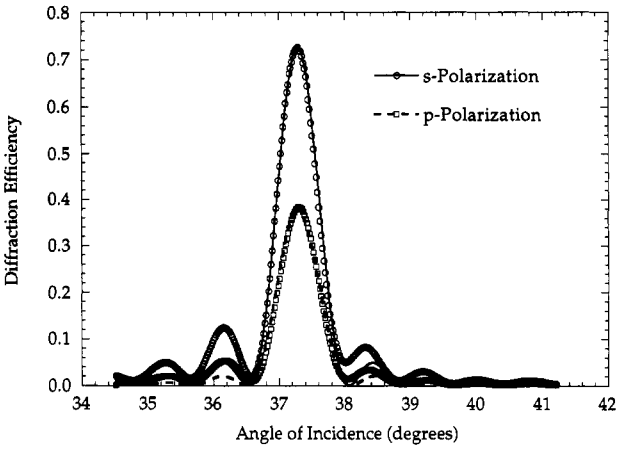

Figure 5. Angular sensitivity plots for a PDLC grating written at 514.5 nm and read with 633 nm using s-polarization (circles) and p-polarization (squares). The solid and dashed curves are fits to the data using coupled-wave theory.

We contrast these results with the grating of Figure 5. This sample was recorded with an identical exposure as that in Figure 4, except the writing wavelength was 514.5 nm. Also, the liquid crystal loading was 26.5 wt %, and the postcuring was done by exposure to room lights over several days. The (external) Bragg angle, measured in this case at 633 nm, was 37.2°. This corresponds to a grating spacing of 0.523 μm, whereas the expected value from eq 2 would be Λ_t = 0.570 μm. Thus, under the conditions of slow postcuring it appears that there is time for appreciable shrinkage of the grating.

The postcuring process also appears to have an effect on the polarization dependence of the diffraction efficiency, which can be seen by fitting Kogelnik's coupled-wave theory[14] to the angular selectivity data. An example of the effect of reading polarization on the measured diffraction efficiency is shown in Figure 5. From coupled-wave theory, the diffraction efficiency is given by

$$\eta = \sin^2(\nu^2 + \xi^2)^{1/2}/(1 + \xi^2/\nu^2) \qquad (3)$$

where $\nu = \pi n_1 L/\lambda \cos\theta$, for s-polarized light, and $\xi = \pi n L \Delta\theta \sin 2\theta_B/\lambda \cos\theta$. L is the physical thickness of the grating, n is the average refractive index, n_1 is the amplitude of the index modulation, λ is the wavelength, θ is the angle of incidence in the sample, and $\Delta\theta = \theta - \theta_B$ is the deviation from the Bragg angle θ_B. The theoretical curves in Figures 4 and 5 are fits of eq 3 to the data, assuming n = 1.52 and using Snell's law to correct for the angle of incidence in the sample. We note that the agreement between theory and experiment is remarkably good even though the index modulation is not strictly sinusoidal as assumed by the theory. The sample thickness L which yielded the best fits was 49.1 μm and 45.8 μm, respectively, for Figure 4a and 4b. In Figure 5 the best fit yielded L = 66.2 μm. Measurements of film thickness on a Sloan Dektak II profilometer yielded 42 and 63 μm, respectively, for the grating samples in Figures 4 and 5. We also note that the index modulation fit parameter n_1 for λ = 633 nm and s-polarized light is 2.80×10^{-3} for Figure 4a and 2.83×10^{-3} for Figure 5. Hence, there is relatively good numerical agreement between independent measurements of the samples, and we conclude that these gratings are well described by coupled-wave theory.

(14) Kogelnik, H. *Bell Syst. Tech. J.* **1969**, *48*, 2909.

According to coupled-wave theory for unslanted gratings,[14] $\nu_p/\nu_s = \cos 2\theta_B$, where ν_p (ν_s) is the coupling coefficient for p-polarized (s-polarized) light, and θ_B is the internal Bragg angle. From the theoretical fits in Figure 5, we find ν_p/ν_s = 0.65 which is in close agreement with the theoretical value of 0.68 determined by the measured (internal) Bragg angle. On the other hand, polarization measurements at 633 nm for the rapid postcure sample of Figure 4 yielded a value of ν_p/ν_s = 0.83, whereas the Bragg angle measurement would predict a value of 0.70. Thus, there is an apparent anisotropy in the grating strength parallel to the grating vector. It is interesting to note that this value was obtained regardless of the liquid-crystal content, even with no liquid crystal in the mixture. Although the liquid crystal enhances the index modulation, it does not appear to modify the anisotropy. We conclude that this is a function of the polymer and may be an anisotropic density resulting from monomer diffusion during the recording process. In fact, the intrinsically anisotropic processes involved in photopolymerization are known to lead to anisotropic diffusion, and the kinetics of this have been studied in detail.[15] As noted above, the same monomer diffusion may be resposible for the ellipsoidal shape of the droplets. Evidently, the slowly postcured sample has enough fluidity to relax this density anisotropy. The rapidly postcured sample locks in the anisotropy in the same way it locks in the grating spacing, not allowing the grating to shrink.

Electric Field Switching. If the gratings in this acrylate system consist of periodic PDLC planes as proposed, we would expect to see a modulation of the diffraction efficiency with an applied electric field, as has been demonstrated in the Raman–Nath regime.[7,8] To test this, we have recorded gratings in samples sandwiched between indium–tin oxide coated glass slides. Preliminary results indicate that the diffraction efficiency can be switched. For example, we have observed a change in peak diffraction efficiency from 20% to ~4% in one sample as the rms voltage is varied from 0 to 400 V. This is accompanied by an equal but opposite change in the zero-order transmittance, indicating that the index modulation has indeed been modified by the field. Interpretation of these results is difficult, however, without knowledge of the nematic director orientation within the droplets. The liquid-crystal molecules may prefer a tangential or normal anchoring at the droplet–matrix interface. These two situations will lead to different nematic director orientations which profoundly affect the electrooptical switching characteristics.[16] Planned NMR experiments should help determine the director configuration in these droplets.[17]

Conclusions

We have demonstrated the holographic formation of Bragg gratings in an acrylate system containing a nematic liquid crystal and have shown that the gratings consist of periodic PDLC planes. Careful control of liquid-crystal loading and postcuring conditions ensure consistent optically clear gratings with high diffraction efficiency. It appears that diffraction efficiencies approaching 100% should be feasible, with angular selectivity widths of <1°.

(15) Krongauz, V. V.; Schmeizer, E. R.; Yohannan, R. M. *Polymer* **1991**, *32*, 1654.
(16) Zumer, S.; Doane, J. W. *Phys. Rev. A* **1986**, *34*, 3373.
(17) Golemme, A.; Zumer, S.; Doane, J. W.; Neubert, M. E. *Phys. Rev. A* **1988**, *37*, 559.

These holographic gratings are formed in a simple single-step process with inexpensive materials and therefore have commercial potential. We are just beginning to explore the features of these PDLC gratings and have discovered a technique to set the gratings for long term stability by rapid postcuring. We note that some initial results have been obtained on electrically switching the diffraction efficiency in these samples, with a change in the peak efficiency by a factor of 5. However, more work needs to be done to understand the internal nematic director configuration of the droplets in relation to the extensively cross-linked matrix and the effects this has on molecular reorientation as a function of field strength.

Acknowledgment. We would like to thank Prof. D. Neckers of The Bowling Green State University in Bowling Green, OH, for the generous gift of Rose Bengal samples as well as helpful discussions. R.L.S., L.V.N., and V.P.T. gratefully acknowledge the support of the Materials Directorate at Wright Laboratory, Wright-Patterson Air Force Base, for their support in this work through U.S. Air Force Contract F33615-90-C-5911.